

# Projector and Camera Calibration Method for Oneshot Scan System with Static Pattern Projector and Monochrome Camera

Hiroshi KAWASAKI<sup>†</sup> (*Member*), Shota KIYOTA<sup>†</sup>, Tatsuya HANAYAMA<sup>†</sup>, Michihiro MIKAMO<sup>†</sup> (*Member*),  
, Ryo FURUKAWA<sup>††</sup>

<sup>†</sup> Department of Information & Biomedical Engineering, Kagoshima University,  
<sup>††</sup> Graduate School of Information Sciences, Hiroshima City University

**<Summary>** In recent years, development on 3D measurement system using a projector and a camera becomes popular. Among them, one-shot scan which requires only a single shot with static pattern becomes important and intensively researched because of the strong demand on capturing moving objects like human. One critical issue for the system is a calibration of the devices, because projectors cannot capture an image, and thus, indirect way to get correspondences between a pixel of the pattern and a 3D point in the scene is required. The typical solution is to capture a special calibration object on which temporally encoded patterns are projected by a projector. However, for one-shot scan, since the pattern is static and cannot be changed, the techniques cannot be applied. In the paper, we extend the plane based method and detection method, with an adaptive binarization and global optimization for efficient separation and detection of overlapped markers. Experimental results are shown to prove the effectiveness of the method.

**Keywords:** calibration, projector calibration, AR toolkit, grid based one-shot scan

## 1. Introduction

Recently, an active stereo method has been used for wide areas, such as inspection, movie creation, etc. The active stereo method measures 3D shapes by projecting lasers or structured lights onto the object and capturing the scene by a sensor. Among them, projector-camera based one-shot scanning becomes popular because of its simplicity, high accuracy, high density and capability of capturing moving objects.

In general, accurate measurement of the active stereo method requires strict calibration of the devices in advance. Although a number of practical solutions are available for camera calibration, there are few for projector. Since the optical system of projectors is the same as that of camera, camera calibration algorithms can be used. However, since projectors cannot capture scenes, correspondences between a pixel of the pattern and a 3D point in the scene should be acquired in an indirect way; e.g., capturing a set of projected patterns by a camera and decoding them. To encode the positional information into the pattern, two methods are known; temporal and spatial methods; note that spatial encoding based scanning methods are called one-shot scan. Although several practical calibration methods for temporal encoding methods

are known<sup>1).2)</sup>, there is few method proposed for spatial encoding methods. Therefore, the solution for the latter methods is proposed in the paper.

Furthermore, as black-white cameras are still fragment used for industrial purposes, we also demonstrate that our system can work with monochrome cameras.

To satisfy the requirements stated above, we propose an efficient calibration method using a planar board with a set of small markers, i.e., AR marker in the paper<sup>3)</sup>. We also propose an extended calibration method for one-shot scan with static pattern and single color<sup>4).5)</sup>. The actual calibration process is as follows. We capture the planar board which AR markers are printed on and the AR markers or static wave pattern are projected by a projector. Those overlapped patterns are efficiently separated by our method, and then, simultaneous calibrations of the camera and the projector is conducted. Contributions of our method are as follows:

1. Distinctive AR marker design to realize better identification for calibration is proposed.
2. To mitigate mis-detection caused by uneven reflection on the board because of the slanted plane, adaptive binarization technique is proposed.
3. Extended calibration for static pattern with single color is proposed.

- Global optimization to efficiently separate the overlapped patterns is proposed.

With the method, easy calibration of projector-camera system is possible without using special devices by simply projecting a static pattern onto the planar board.

## 2. Related research

Historically, temporal coding technique with 3D calibration objects (typically a square box) has been conducted to calibrate projector-camera system<sup>1)</sup>. One major drawback of the method is a preparation of calibration objects. For example, construction of the box with 1m high for human body scan is practically difficult. Recently, plane based methods are proposed for the solution<sup>6)</sup>. Since the methods utilize the algorithm for camera calibration, it usually requires 20 to 40 shots of the plane with different poses. Further, since the methods are based on temporal coding, multiple projections are required to get correspondences for each shot, and thus, more than hundred images are necessary for calibration.

To avoid such a complicated task, spatial methods become popular<sup>7)</sup>. With the method, checker board pattern is projected onto the planar board and the pattern is detected by common libraries. Since entire pattern should be captured for stable detection and it is not easy to project the entire pattern onto the limited size of the board, the quality of the calibration is unstable. There are several attempts which calibrate a projector with special approaches<sup>8),9)</sup>. Audet *et al.* propose a method using a local markers with feedback from a camera<sup>8)</sup> and Drareni *et al.* propose a self-calibration method using a marker-less planar object<sup>9)</sup>. Our technique also provides the alternative solution.

Recently, one-shot scanning methods where a single color and a static pattern are used have attracted many people, because of its stability and robustness<sup>4),5),10)</sup>. Since the system usually consists of a static pattern, the pattern cannot be changed for the calibration process and it makes the calibration significantly difficult. We also propose a solution for this case in the paper.

## 3. Overview

### 3.1 System configuration

The configuration of the camera, the projector and the calibration object for the proposed method is shown in **Fig. 1**. The planar board with a static pattern is used as the calibration object. Then, the static pattern is also projected onto the board to calibrate the projector-

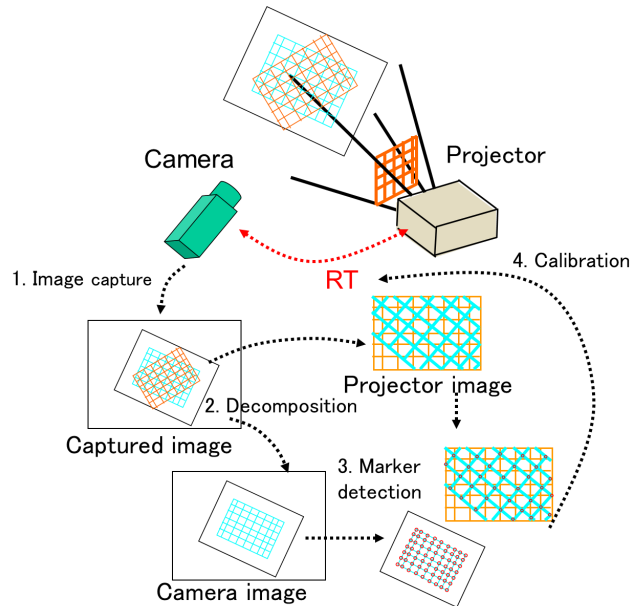


**Fig. 1** Setup of Camera and Projector

camera system. The images used for the calibration are obtained by capturing the planar board. Since two patterns are overlapped each other on the board, the robust separation algorithm of the pattern is required. Note that, for the image capturing process, it is preferable to widely move and rotate the planar board to increase the variation of the depths of feature points for better calibration; such condition makes it difficult to achieve robust marker detection. The efficient solution for partially captured pattern and/or strong specular reflection by projector is proposed in the paper.

### 3.2 Algorithm

The proposed method is divided into four steps as shown in Fig. 1. First, images required for calibration are captured by the camera. In the method, the AR marker is printed on the planar board and the AR marker or the static pattern is projected onto the board by the projector. Since the calibration cannot be done with the images overlapped with two patterns, those patterns should be decomposed. Therefore, in the second step, decomposition of two patterns is efficiently conducted by using the subtle differences of the intensity of the patterns. In the method, one of the patterns is first detected and extracted, and then, the other pattern is retrieved afterwards using the first extracted pattern. In the third step, we detect markers from each patterns. In the step, auto-detection of the marker is done by using ARToolKit<sup>3)</sup>, respectively. At the fourth step, using the coordinate of the detected pattern, intrinsic calibration of the camera



(a) Classic AR markers<sup>3)</sup>



(b) Our original AR markers

**Fig. 2** Example of AR markers

and the projector as well as the relative position ( $R$  and  $t$ ) of the camera and the projector are estimated. They are further optimized by minimizing the reprojection error.

## 4. Detection of markers for AR marker projection

### 4.1 Distinctive pattern design and color

To utilize the common libraries for pattern detection, previous methods use a checker pattern<sup>7)</sup>. To mitigate the severe restriction on capturing process where the entire pattern must be captured, several solutions can be considered. For example, Matlab allows users to manually select valid correspondences. Another approach is to put special markers near the center of the pattern. In the paper, we propose a full automatic solution using a pattern which consists of a number of small independent markers. In our method, we used 63 different AR markers aligned  $7 \times 9$ . However, the calibration accuracy will be drastically reduced, if ID of the marker is wrongly detected. In order to keep enough uniqueness for all the markers, new AR markers are designed. Standard markers usually use a picture for easy detection as shown in **Fig. 2(a)**, whereas our AR marker consists of barcode-like 2D marker as shown in **Fig. 2(b)**. The markers were created using a 0/1 flags within a  $5 \times 5$  block to maximize the minimum Hamming distance between the markers. We use the center of gravity of four corners of the detected AR marker for stable calibration in the following steps.

In the method, two patterns are required: The pattern for a planar board and the pattern for projection. Note that original AR markers consist of two colors, such as black and white, and thus, if original patterns are overlapped each other, output colors become only black and white and cannot be decomposed as shown in **Table 1**. Therefore, we introduce gray color instead of black for

**Table 1** Intensity of reflectance of original pattern.

Image Board Intensity	Projector	
	Dark	Bright
Dark	0	0
Bright	1.0	0

**Table 2** Intensity of reflectance of our method.

Image Board Intensity	Projector	
	Dark	Bright
Dark	0.35	0.07
Bright	1.0	0.2

the pattern. **Table 2** shows an example of color assignment for each pattern and their mixtures. We can confirm that four possible combinations represent their own unique colors.

Since intensity of reflected color is proportional to a multiplication of incident light and surface color, SN ratio (color difference to distinguish regions) of dark region is worse than bright region as the blue line in **Fig. 3**. To solve the problem, we intentionally use the saturation of CCD, which is normally avoided, to create non-linearity of response function as the red line in **Fig. 3**. We can confirm that minimum difference value between colors is doubled from 0.13 to 0.26.

In our implementation, the dark parts with the intensity of 200 are used for the planar board pattern, and the intensity of 100 is used for the projector pattern as shown in **Fig. 4** when intensity of 255 represents white color.

### 4.2 Adaptive binarization for the first pattern

**Figure 5(a)** and **6(a)** are examples of captured images. Since intensities of the patterns are intentionally biased,

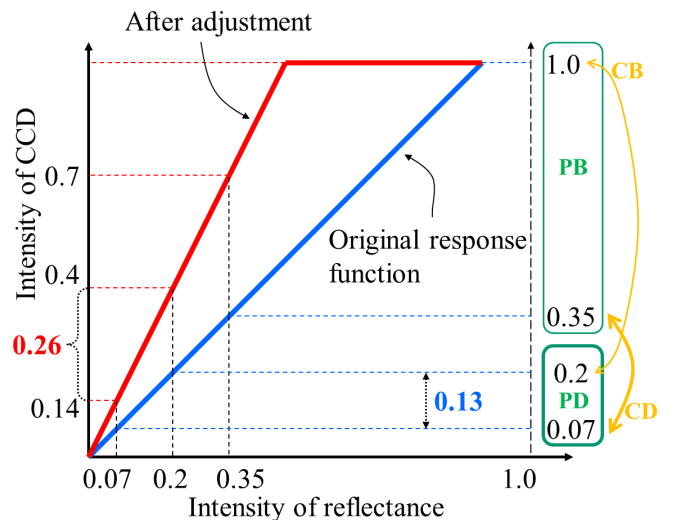


**Fig. 3** Response function for two different albedo.

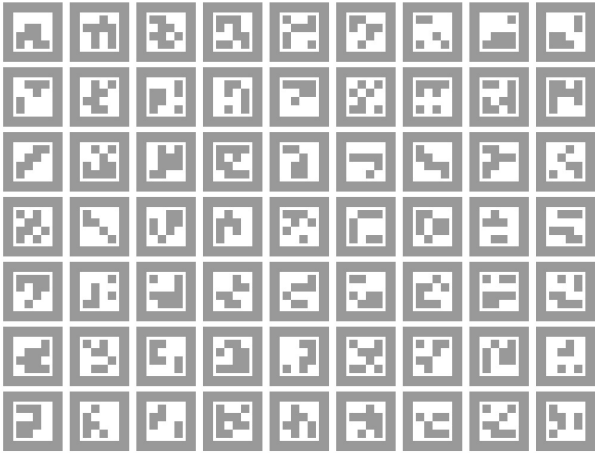


**Fig. 4** Calibration patterns with our original AR markers

we can observe four different colors, which are the combinations of two colors from the board and projection, respectively. Although there are four colors, we can set the specific threshold to separate the pattern; note that it is possible only for one of two patterns, which can be easily understood by right-axis in Fig. 3. In addition, since the orientation of the planar board is widely changed at each capture, the captured image has uneven brightness especially when a direction of the surface becomes parallel to the view direction. Therefore, if the binarization was processed with single threshold for the entire image, the process will fail as shown in Fig. 5(b).

To solve this problem, adaptive binarization is applied. Specifically, after extracting the small number of AR markers with the global threshold, adaptive binarization is carried out by individually binarizing each marker. The positions of each marker can be localized by using the board position in 3D space, the position is estimated by the initially retrieved small number of markers. Note that a simple adaptive approach such as dividing the image into rectangular blocks usually fails because of drastic change of brightness on the board. As shown in Fig. 5(c), we can detect only 9 AR markers from the initial binarization result of Fig. 5(b). However, using the valid AR markers in Fig. 5(c), the area was expanded and binarization was successfully performed over the entire field as shown in Fig. 5(d).

#### 4.3 Second pattern detection by global optimization

Unlike the first pattern, the second pattern theoretically cannot be binarized by a single threshold; the reason can also be understood by right-axis in Fig. 3. To solve the problem, we propose a technique utilizing the

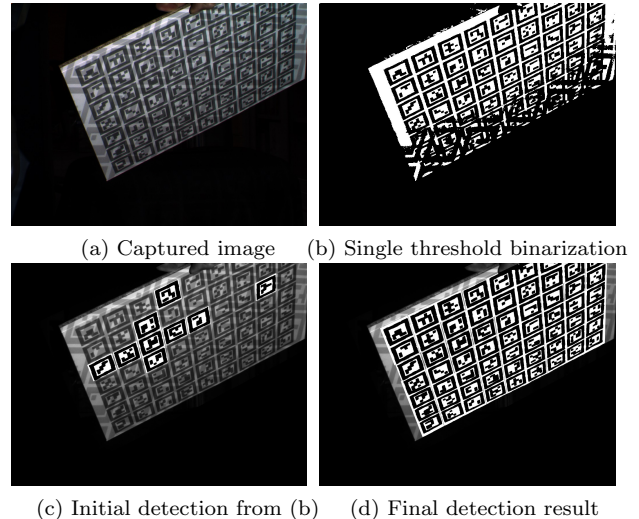


**Fig. 5** Iterative process of adaptive binarization method.

first pattern binarization result with the following approach. We first make two masks for both negative and positive sides from the first binarization result as shown in Fig. 6(b). Then, we apply the masks to the original image to decompose the image into two as shown in Fig. 6(c) and (d), respectively; note that binarization is possible with a single threshold on those decomposed images. To improve the result, we also apply the adaptive binarization method. Results are shown in Fig. 6(e) and (f). Finally, the two images are merged into one as shown in Fig. 6(g). Since the image contains considerable errors especially near the boundary of the pattern, graph cut(GC) is conducted for refinement<sup>11</sup>). Then, AR markers are detected from the image and the result is shown in Fig. 6(h).

## 5. Extended technique for one-shot scan

The method proposed in the previous section can be used for the system with the video projector where the projected pattern can be arbitrarily changed, however, the technique cannot be used for the actual one-shot system which usually consists of a special projector with a static pattern like Kinect<sup>10</sup>). Therefore, in this section, we propose a method which can be used in one-shot scanning technique, especially static, single-color and grid pattern system<sup>4),5)</sup>; note that although the technique is not fully generalized for all the static patterns, since such a grid based one-shot scanning system becomes popular because of its ability to capture fast moving objects, we believe that the technique still has enough contribution to the community.

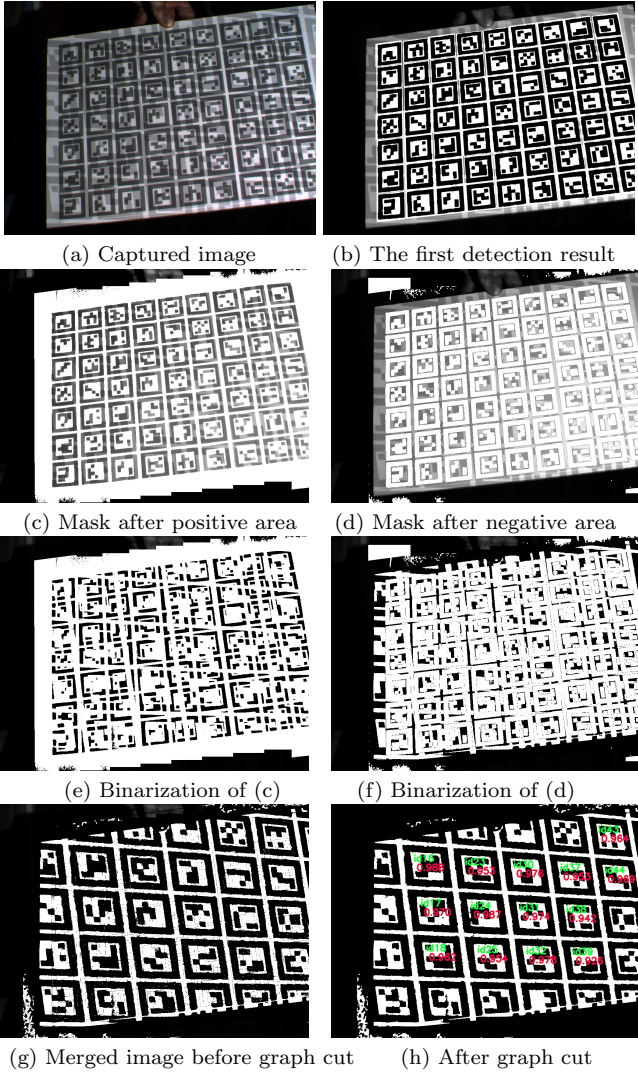


Fig. 6 The second pattern binarization result with graph cut

### 5.1 One-shot scanning method with wave pattern

One-shot scanning method can reconstruct shape just from a single captured image as shown in Fig. 7(a). Since the method is suitable for capturing moving objects like a human or fluid, the methods are attracting many people<sup>(4),5),10)</sup>. To realize one-shot scan, in order to achieve both accuracy and robustness, there is an open issue that how to efficiently embed the information of feature points into the pattern. Among various techniques which have been proposed for it, we adopt the recently proposed technique which uses static and a single color wave pattern<sup>5)</sup> for the paper; the actual pattern is shown in Fig. 8. With the technique, by using different phases for vertical and horizontal directions as shown in Fig. 7(b), it achieves robust 3D reconstruction than before.

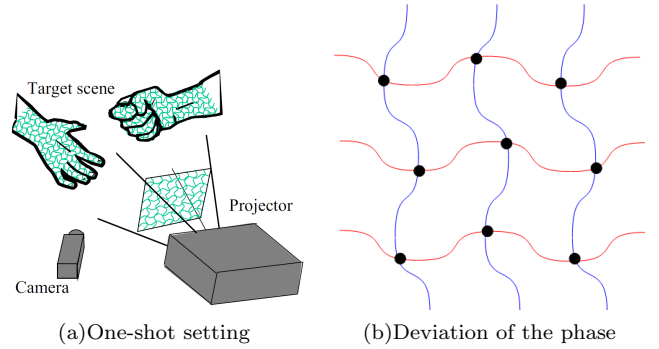


Fig. 7 Grid based one-shot scanning method

### 5.2 Basic principle of calibration

There is a fundamental problem on calibrating for one-shot scanning with a static pattern. In general, oneshot scanning methods find a corresponding point along epipolar line, i.e., 1D search, which is calculated and drawn by using extrinsic parameters. However, the extrinsic parameters are usually calibrated by using corresponding points and this is not known yet. This is a typical chicken and egg problem and the solution is required. In the paper, we use the information that the projected pattern consists of grid shapes. The actual method is as follows. First we extract a grid pattern using intensity differences between the projected pattern and the marker printed on the calibration board. Then, we rectify the extracted projected pattern so that the vertical and horizontal lines of the grid pattern become parallel to the axes of image coordinate. Once such a regular grid pattern is made, we can conduct template matching to find correspondences with 2D search using a large window, which helps a robust search. By using the retrieved corresponding points, extrinsic calibration is possible.

### 5.3 Pattern separation with color information

In the paper, as for the pattern for reconstruction, the static wave pattern with a single color as shown in Fig. 8 is used. The pattern is projected to the calibration board where the AR markers are printed. In this method, color information is used for pattern separation. Fig. 9(a) shows the actual captured image and Fig. 9(b) and (c) show the separated images, respectively. To detect the marker for the separated pattern of AR marker on the board, the technique described in the previous section is used. For the wave pattern, a detection method will be explained in the next section.

### 5.4 Wave pattern detection, editing and selection

First, grid patterns are detected by the method proposed by Sagawa et al.<sup>12)</sup> and the example of detection

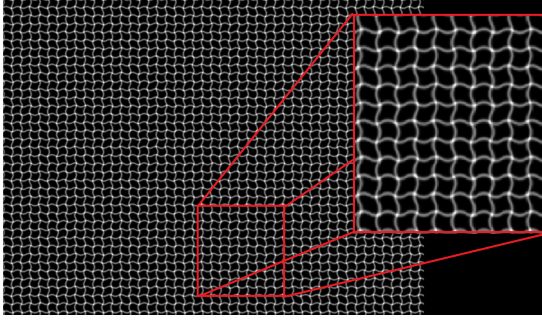
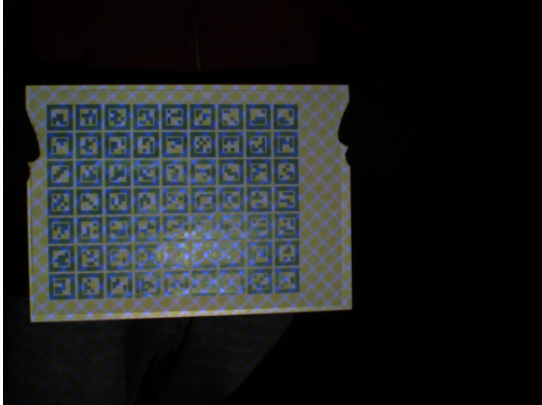
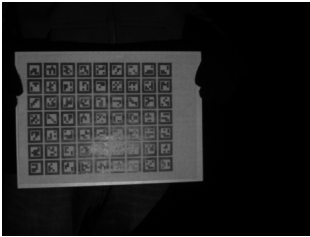


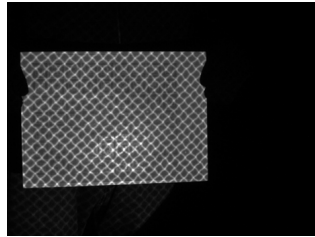
**Fig. 8** Wave pattern with a single color



(a) Captured image



(b) AR marker image

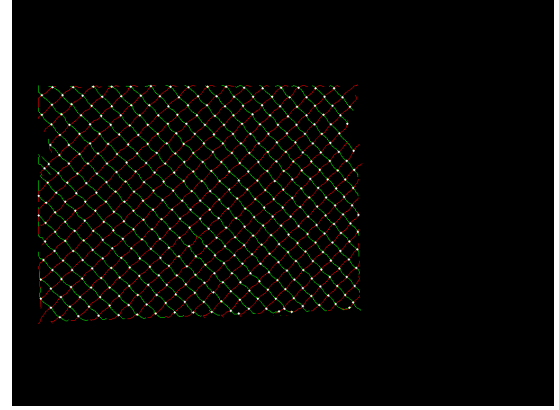


(c) wave pattern image

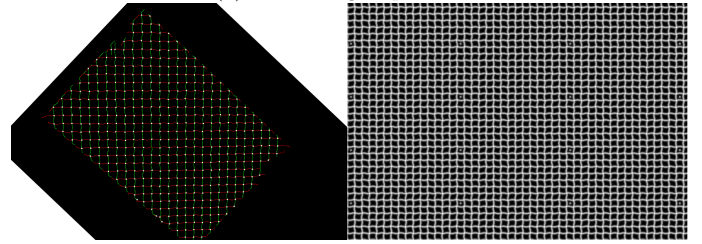
**Fig. 9** The actual captured image (a) and the separated images(b) and (c)

result is shown in **Fig. 10(a)**. Since the projected pattern is a grid pattern, the detected pattern can be easily rectified as shown in Fig. 10(b). After rectification, although two degrees of freedom of the vertical and horizontal direction remain, they are easily determined by a template matching.

Since AR markers are distinctively printed on the board, wrong lines are detected at some parts and actual lines are not detected in other parts during the pattern detection process as shown in **Fig. 11**. Since such erroneous detections result in failure on rectification and template matching, we propose a GUI system where those errors are manually edited and corrected for the solution. GUI system works as follows. First, it reads the correspondence information from the detection results and visualizes them on both the projected pattern and the captured image. Since the pattern is grid-shaped, it is



(a) Detected grid pattern



(b) Rectified grid pattern

**Fig. 10** Wave pattern detection and rectification results

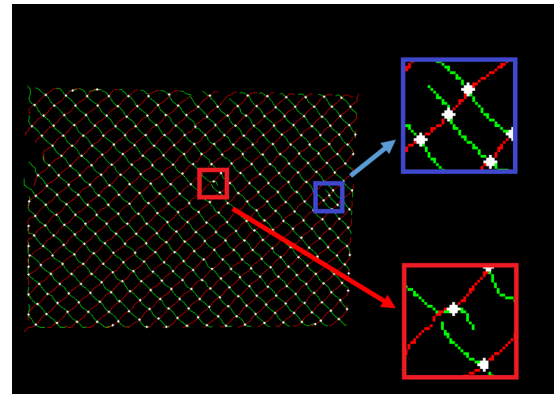


**Fig. 11** Wave line detect

easy to find wrong correspondences by human, and thus, user can select them by using a pointing device to remove them. Furthermore, to find correct correspondences between patterns and captured image, we add several special dots in the pattern as shown in **Fig. 12**. Based on those small improvements, the system finally becomes reliable even if the calibration condition is not ideal.

## 6. Calibration

### 6.1 Estimation of the initial parameter

The intrinsic calibration of the camera is the same as Zhang's method. The intrinsic calibration of the projector is conducted according to the 3D position of AR marker calculated by the result of the camera calibration. The extrinsic parameters are also obtained through the process, however, the estimated parameter here is re-

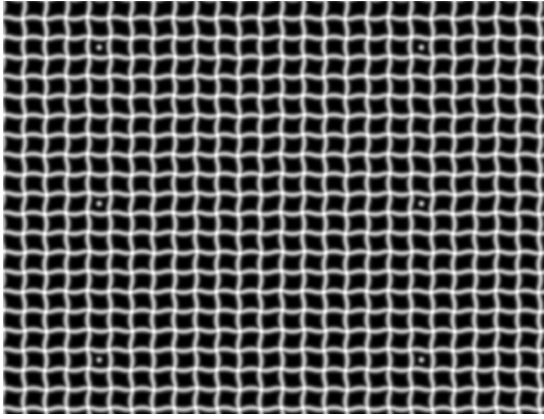


Fig. 12 wave pattern dot

dundant since they are independently estimated for the camera and the projector. Therefore, they are used as the initial value to re-estimate the precise parameter as explained in the next section.

## 6.2 Accurate estimation by bundle adjustment

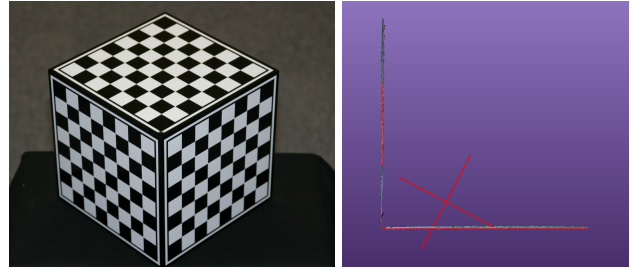
If we have  $n$  images for input, the number of the extrinsic parameter, which includes three for rotation and three for translation for each, is  $2 \times 6n$ . However, since the relative position between projector and the camera is fixed, not all parameters are independent and the number of unknown parameter is  $6n + 6$ . With such a condition, parameters are efficiently optimized by using the bundle adjustment. In addition, the proposed method optimizes the focal length of the camera and the projector (four parameters) at the same time. Therefore, the number of parameter is  $6n + 6 + 4$ . The sum of the reprojection error for the camera and the projector is calculated by the following equation.

$$E = \sum_{i=0}^n \sum_{a=0}^p (E_c + E_p), \quad (1)$$

where  $n$  is the number of images,  $p$  is the number of unique points,  $E_c$  is the reprojection error of the camera, and  $E_p$  is the reprojection error of the projector. With this method, since the position between the camera and the projector can be estimated as the consistent parameters, accuracy and stability of the calibration are greatly improved.

## 7. Experiment

To confirm the effectiveness of the proposed method, we conducted the experiments with a static pattern of the monochrome AR, and the pattern with the wave grid.



(a) 90 angles box (b) Reconstruction result

Fig. 13 Comparison of the accuracy of the calibration box.

Table 3 Shape accuracy compared to ground truth.

	angles(degree)	RMSE(mm)
Grand truth	89.95	0.67
Ours	89.70	0.56

Table 4 Results of marker detection and identification.

	Num. of shots	Num. of detection	Num. of correct ID	
			$C > 0.8$	$C > 0.9$
Original AR	40	2,144	1,636	583
Optimized AR	40	2,337	2,298	1,204

\*  $C$  denotes the confidence ratio, larger than 0.9 is preferable.

### 7.1 Monochrome AR pattern

In this experiment, we use EPSON EP-110 for the video projector and Grasshopper PointGrey Inc. for CCD camera as shown in Fig. 7(a). 3D shapes are reconstructed by using temporal encoding method<sup>13</sup>. Experimental results and evaluations are explained in the followings.

#### 7.1.1 Recover the shape of box with 90 angles

First, we recover the shape of box with 90 angles as shown in Fig. 13(a). The calibration result using the special calibration box with Gray code pattern was applied as the ground truth. The reconstruction result is shown in Fig. 13(b) and the numerical results are shown in Table 3. We can confirm that our results are almost same as the ground truth.

#### 7.1.2 Detection accuracy verification of optimization marker

Next, the accuracy of detection are identification was compared between original AR and optimized one in Fig. 2(a). As shown in Table 4, although there is a little difference on detection number, we can confirm that identification accuracy is greatly improved with our marker.

#### 7.1.3 Accuracy compared with the previous work

Then, the results using the checker pattern<sup>14</sup>, and the AR marker were compared. As shown in Table 5, we can confirm that our monochrome pattern can detect more valid shots than checker board pattern, resulting in better accuracy in reconstruction.

**Table 5** Comparison to checker board pattern<sup>14</sup>.

	Num. of shots	Num. of valid shot	Num. of detect pts.	RMSE (pix.)	Angle (deg.)
Checker <sup>14</sup>	40	27	3,360	1.84	87.53
Proposed	40	39	1,972	1.55	88.63

**Table 6** Comparison of different input numbers.

	1) Single threshold	2) Proposed (w/o GC)	3) Block (with GC)	4) Proposed (with GC)
Shots	40	40	40	40
Detect pts.	321	1,316	1,327	1,741
RMSE(mm)	4.61	0.62	0.60	0.62
90 deg.	28.166	90.99	90.82	90.41
Shots	20	20	20	20
Detect pts.	77	131	295	627
RMSE(mm)	20.40	1.02	1.05	0.70
90 deg.	156.80	79.44	85.90	90.04

### 7.1.4 Accuracy verification of the difference of separation techniques

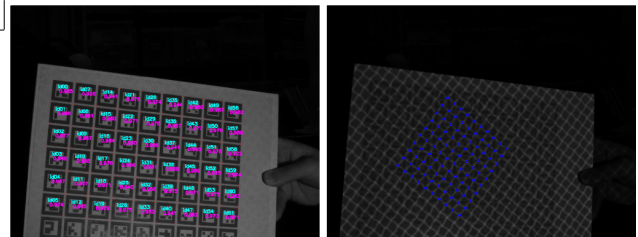
Finally, we test the effectiveness of the proposed method with various conditions using the same pattern; 1) without adaptive binarization using a single threshold, 2) our adaptive binarization without graph cut, 3) adaptive binarization with predefined 2D block with graph cut and 4) our binarization method with graph cut. As shown in Table 6, we can confirm that the adaptive method greatly increases the detection number and improves calibration accuracy. We can also confirm that if we have enough number of input such as 40, all the adaptive methods realize enough quality, whereas only our method can achieve high quality with small number such as 20.

## 7.2 Wave pattern

Then, experiments with the wave pattern were conducted. We used a diffractive optical element (DOE) with a laser projector as for the pattern projector and a PointGrey camera for imaging device; note that the DOE projector cannot change its pattern. First, we detect feature points by using the techniques described in Section 4 and 5 from the separated images. The examples of detection results are shown in **Fig. 14**(a) and (b). By using the detected points, calibration is conducted and results are shown in Table 7. Reprojected points using the calibration parameters are shown in **Fig. 15**(a) where red points represent detected point and blue points represent reprojected points and reconstructed cube with 90 degree corner is shown in Fig. 15(b). From the result, we can confirm that the both AR marker and wave pattern are correctly detected with our method. Furthermore, we can confirm that the reprojection error is also suffi-

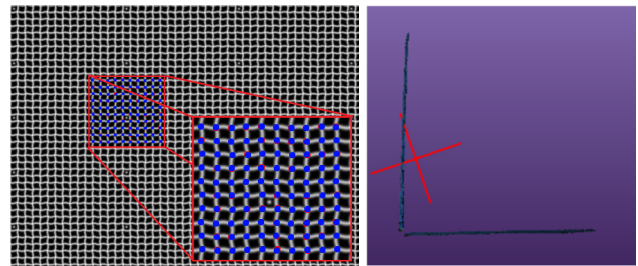
**Table 7** Calibration result using wave pattern

Num. of shots	Num. of valid shot	Num. of detect pts.	RMSE (pix.)	Angle (deg.)
30	22	3,614	0.90	87.6291



(a) Detection results from the camera image

(b) Detection results from the projector image

**Fig. 14** The examples of detection results

(a) Reprojection result

(b) Reconstruction result

**Fig. 15** Wave grid pattern one-shot scanning results

ciently small value, proving that the correct corresponding points are obtained. We can also confirm that the estimated extrinsic parameter is enough accurate from the reconstructed shape which has almost 90 degrees at the corner.

## 8. Conclusion

In the paper, we propose a practical and accurate calibration method for monochrome AR markers and static wave pattern. Since it is not required to detect the entire pattern for calibration, freedom on configuration of the camera and the projector and movement of the planar board are greatly improved, resulting in fast and easy data acquisition process, which realizes accurate calibration. Experiments were done to show the successful results on calibration. In the future, calibration of multiple sets is planned.

## Acknowledgment

This work was supported by SCOPE No.151310005 of Ministry of Internal Affairs and Communications in Japan.

## References

- 1) R. Furukawa, H. Kawasaki: "Uncalibrated Multiple Image Stereo System with Arbitrarily Movable Camera and Projector for Wide Range Scanning," Proc. of The Fifth International



- Conference on 3-D Digital Imaging and Modeling (IEEE Conf. 3DIM), pp. 302–309 (2005).
- 2) H. Kawasaki, Y. Ohsawa, R. Furukawa, Y. Nakamura: “Dense3d Reconstruction with An Uncalibrated Active Stereo System,” Proc. of The 7th Asian Conference on Computer Vision (ACCV06), vol. 2006-ACCV06, pp. 882–891 (2006).
  - 3) H. Kato, M. Billinghurst: “Marker Tracking and HMD Calibration for A Video-Based Augmented Reality Conferencing System,” Proc. of The 2nd International Workshop on Augmented Reality (IWAR 99), pp. 85–94 (1999).
  - 4) R. Sagawa, Y. Ota, Y. Yagi, R. Furukawa, N. Asada, Hiroshi Kawasaki: “Dense 3D Reconstruction Method Using A Single Pattern for Fast Moving Object,” Proc. of International Conference on Computer Vision (ICCV ‘09), pp. 1779–1786 (2009).
  - 5) R. Sagawa, K. Sakashita, N. Kasuya, H. Kawasaki, R. Furukawa, Y. Yagi: “Grid-based Active Stereo with Single-Colored Wave Pattern for Dense One-shot 3D Scan,” Proc. of Second Joint 3DIM/3DPVT Conference: 3D Imaging, Modeling, Processing, Visualization and Transmission, pp. 363–370 (2012).
  - 6) M. Kimura, M. Mochimaru, T. Kanade: “Projector Calibration using Arbitrary Planes and Calibrated Camera,” Proc. of IEEE CVPR Workshop on Projector-Camera Systems (ProCams), Vol. CD-ROM, pp. 1–1 (2007).
  - 7) S. Kiyota, H. Kawasaki, R. Furukawa, R. Sagawa: “Efficient Projector Calibration Method using Plane with Checkerboard Pattern,” Information Processing Society of Japan (IPSJ) Technical Report, Vol. 2012-CVIM-180, pp. 1–8 (2012).
  - 8) S. Audet, M. Okutomi: “A User-Friendly Method to Geometrically Calibrate Projector-Camera Systems,” Proc. of The 6th IEEE International Workshop on Projector-Camera Systems (Procams2009), pp. 47–54 (2009).
  - 9) J. Drareni, P. Sturm, S. Roy: “Projector Calibration Using a Markerless Plane,” Proc. of The International Conference on Computer Vision Theory and Applications, Vol.2, pp. 377–382 (2009).
  - 10) Microsoft, “Xbox 360 Kinect,” <http://www.xbox.com/en-US/> (2010).
  - 11) Y. Boykov, O. Veksler R. Zabih: “Efficient Approximate Energy Minimization via Graph Cuts,” IEEE Trans. on Pattern Analysis and Machine Intelligence, Vol. 20, No. 12, pp. 1222–1239, (2001).
  - 12) R. Sagawa, K. Sakashita, N. Kasuya, H. Kawasaki, R. Furukawa, Y. Yagi: “Grid-Based Active Stereo With Single-Colored Wave Pattern for Dense One-Shot 3D Scan,” Proc. of The 2nd International Conference on 3D Imaging, Modeling, Processing, Visualization and Transmission (3DIMPVT), pp. 363–370 (2012).
  - 13) R. Furukawa, H. Kawasaki: “Self-Calibration of Multiple Laser Planes for 3D Scene Reconstruction,” Proc. of The 3rd International Symposium on 3D Data Processing, Visualization and Transmission (3DPVT), pp. 200–207 (2006).
  - 14) S. Totsuka, R. Furukawa, H. Kawasaki: “Precision Improvement Method for Phase Shifting based Projector-Camera Stereo System Using Response Function,” Proc. of Meeting on Image Recognition and Understanding 2009 (MIRU2009), pp. 1594–1599 (2009).

(Received March 9, 2015)

(Revised May 15, 2015)



### Hiroshi KAWASAKI (*Member*)

He received his Ph.D in engineering from University of Tokyo, Japan, in 2003. Currently, he is an professor at the Department of Information and Biomedical Engineering, Kagoshima University, Japan. His research interests include computer vision and computer graphics.



### Shota KIYOTA

He received his Master of Engineering from the Department of Information and Biomedical Engineering, Kagoshima University, Japan, in 2013. His research interests include computer vision.



### Tatsuya Hanayama

He received his Bachelor of Engineering from the Department of Information and Biomedical Engineering, Kagoshima University, Japan, in 2014. Currently, he is an Master course student at the Department of Information and Biomedical Engineering, Kagoshima University, Japan. His research interests include computer vision.



### Michihiro MIKAMO (*Member*)

He received his Ph.D in engineering from Hiroshima University, Japan, in 2013. Currently, he is an assistant professor at the Department of Information and Biomedical Engineering, Kagoshima University, Japan. His research interests include computer graphics and computer vision.



### Ryo FURUKAWA

He received his Ph.D in engineering from Nara institute of Science and Technology, Japan, in 1996. Currently, he is an associate professor at the Graduate School of Information Sciences, Hiroshima City University. His research interests include computer vision and computer graphics.